

## SUPPLEMENTAL MATERIAL

### Supplemental Methods

#### *Animals*

Analysis of normal development at different time points (E10.5 to P0) was carried out on embryos harvested from timed pregnancies in CD-1 mice (Jackson Laboratory). For each embryonic stage of development, we collected micro-CT data sets for three individual specimens while seven specimens were necessary to evaluate the various staining conditions we outlined in our manuscript for the single postnatal time point we investigated. Staging was confirmed morphologically at the time of dissection and on 3D volume renderings. *PlexinD1* mutant mice have been described previously (1) and a single *plexinD1*-null embryo and its wild type littermate control were utilized for the corresponding studies.

#### *Image Analysis*

The 3D micro-CT image volumes generated at the scanner are 16-bit data files of approximately 300 MB, and these were downsampled to 8-bit data (~ 150 MB) in order to make them easier to work with in the visualization software. We employed several image analysis tools for qualitative inspection of the image data and for quantitative measurements of image intensity and structural dimensions. These tools include the open source software packages MicroView (GE Healthcare), ImageJ (NIH), and OsiriX ([www.osirix-viewer.com](http://www.osirix-viewer.com)). Three visualization methods were used in this study: multi-planar reformatting (MPR), volume rendering (VR), and maximum intensity projection (MIP). Real-time interactive 3D visualization using these methods was enabled by running a 64-bit version of OsiriX on a Mac Pro workstation (Apple Computer, Inc.)

having two 3 GHz Intel Xeon Dual-Core processors, 12 GB RAM, and a high-end graphics card (512 MB VRAM).

The 3D isotropic nature of the micro-CT image data (voxel size =  $16 \times 16 \times 16 \mu\text{m}^3$ ) permits MPR at arbitrary oblique planes without significant loss of resolution, although a minor amount of smoothing occurs due to necessary interpolation between voxels. MPR thus enables visualization of heart and vascular structures at ideal orientations, permitting qualitative inspection of the internal anatomy and also quantitative thickness measurements of structures of interest. In addition, VR and MIP techniques provide complementary qualitative information. While both are based on ray tracing algorithms, VR makes use of depth cues, shading, and texturing to display a 3D representation of the data, whereas MIP reveals the brightest internal structures. By changing the image display settings, such as the window width and level, different aspects of the data can be emphasized. This is especially true for VR, and the VR images shown in this paper were generated in OsiriX using the following settings: muscle/bones color look up table, logarithmic inverse opacity table, shading coefficients: ambient = 0.15, diffuse = 0.90, specular = 0.30, specular power = 15.0, and various window width/level values.

## References

1. Gitler AD, Lu MM, Epstein JA. PlexinD1 and semaphorin signaling are required in endothelial cells for cardiovascular development. *Dev Cell*. 2004;7(1):107-116.

**Supplemental Table 1.** Values of parameters  $C_0$  and  $D$ , obtained by curve fitting Equation 1 to the time course of iodine diffusion as measured at position  $x$  in the brain stem of each mouse in Figure 2. Nominal  $[I]$  refers to the presumed iodine concentration in each bath of Lugol's solution.

Lugol's solution	nominal $[I]$ (mM)	$x$ ( $\mu\text{m}$ )	$C_0$ (mM)	$D$ ( $\text{mm}^2/\text{s}$ )
saturated 25%	> 246.5	560	1421	$5.15 \times 10^{-6}$
isotonic 25%	246.5	563	913.5	$5.99 \times 10^{-6}$
isotonic 12.5%	123.25	683	717.1	$3.95 \times 10^{-6}$

## Supplemental Figure Legends

**Supplemental Figure 1.** Calibration curve of micro-CT image intensity from serial dilutions of Lugol's solution shows a highly linear relationship between iodine concentration and X-ray attenuation. Serial dilutions of 100% Lugol's solution were made using de-ionized water and were scanned as phantoms. Each point corresponds to the mean intensity of a ROI drawn on the reconstructed images of each phantom. Standard deviations of the means were only slightly larger than the size of the plotted symbols. The fitted solid line demonstrates the highly linear behavior ( $R^2 = 0.9999$ ), as expected for X-ray attenuation by iodine. The line has a slope (K factor) of 5.37 HU/mM and an offset of 10.5 HU. This offset is well within the standard deviation of intensity values around the value of zero, which is the intensity of pure water on the Hounsfield scale. Unstained, non-fatty tissues have intensity values very close to that of water. Therefore, to convert images (HU) into maps of apparent iodine concentration (mM), we can apply the following formula to each pixel in the image:  $\text{mM} = (\text{HU} - 10.5)/5.37$ .

**Supplemental Figure 2.** Variations in display settings demonstrate the effectiveness of iodine staining for visualizing multiple anatomic features from a single micro-CT data set. **(A)** False color VR image of a wild type E17.5 embryo, windowed to show the entire embryo, gives excellent superficial detail. **(B, C)** Alterations in window settings highlight vasculature and internal organs. **(D)** MIP image highlights vascular patterning.

**Supplemental Figure 3.** Quantification of the vessel diameters by micro-CT is comparable to measurements taken from histological sections. Cross-sections through the

thoracic aorta result in an oval shape in embryos at E17.5. The vessel diameters were measured along the long- and short-axis of this oval just posterior to the carina as shown in panels (A) and (B) (micro-CT MPR and H&E stained section, respectively). There is no significant difference in the mean diameters as measured by either technique (C) (n=3 specimens for each measurement) (Es, esophagus; Br, bronchus).

## **Supplemental Movie Legends**

**Supplemental Movie 1.** Iodine staining enables visualization of cardiovascular development and multiple anatomic features in embryonic and neonatal mice by micro-CT. The movie shows sagittal slices through a micro-CT data set of an iodine-stained wild type mouse embryo (stage E10.5), demonstrating very little inter-tissue contrast yet still providing good delineation of cardiovascular structures. The micro-CT data were reconstructed at an isotropic resolution of 16  $\mu\text{m}$ , and are displayed with pixel interpolation performed in OsiriX software.

**Supplemental Movie 2.** Iodine staining enables visualization of cardiovascular development and multiple anatomic features in embryonic and neonatal mice by micro-CT. The movie shows sagittal slices through a micro-CT data set of an iodine-stained wild type mouse embryo (stage E11.5), demonstrating good inter-tissue contrast, although not as much as that of later stage embryos. The micro-CT data were reconstructed at an isotropic resolution of 16  $\mu\text{m}$ , and are displayed with pixel interpolation performed in OsiriX software.

**Supplemental Movie 3.** Iodine staining enables visualization of cardiovascular development and multiple anatomic features in embryonic and neonatal mice by micro-CT. The movie shows sagittal slices through a micro-CT data set of an iodine-stained wild type mouse embryo (stage E13.5), demonstrating high inter-tissue contrast. The

micro-CT data were reconstructed at an isotropic resolution of 16  $\mu\text{m}$ , and are displayed with pixel interpolation performed in OsiriX software.

**Supplemental Movie 4.** Iodine staining enables visualization of cardiovascular development and multiple anatomic features in embryonic and neonatal mice by micro-CT. The movie shows sagittal slices through a micro-CT data set of an iodine-stained wild type mouse embryo (stage E15.5), demonstrating high inter-tissue contrast. The micro-CT data were reconstructed at an isotropic resolution of 16  $\mu\text{m}$ , and are displayed with pixel interpolation performed in OsiriX software.

**Supplemental Movie 5.** Iodine staining enables visualization of cardiovascular development and multiple anatomic features in embryonic and neonatal mice by micro-CT. The movie shows sagittal slices through a micro-CT data set of an iodine-stained wild type mouse embryo (stage E17.5), demonstrating high inter-tissue contrast. The micro-CT data were reconstructed at an isotropic resolution of 16  $\mu\text{m}$ , and are displayed with pixel interpolation performed in OsiriX software.

**Supplemental Movie 6.** Iodine staining enables visualization of cardiovascular development and multiple anatomic features in embryonic and neonatal mice by micro-CT. The movie shows sagittal slices through a micro-CT data set of an iodine-stained wild type mouse neonate (stage P0), demonstrating high inter-tissue contrast. The micro-CT data were reconstructed at an isotropic resolution of 32  $\mu\text{m}$ , and are displayed with pixel interpolation performed in OsiriX software.



### **Supplemental Movie 7**

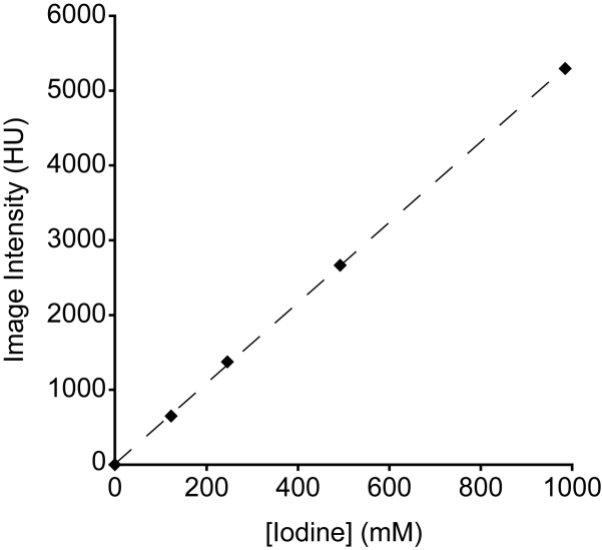
Three-dimensional volume rendered images of ventricles and great vessels in a wild type E17.5 mouse embryo reveals normal conotruncal anatomy and arch patterning.

### **Supplemental Movie 8**

Three-dimensional volume rendered images of ventricles and great vessels in an E17.5 *PlexinD1* mutant mouse embryo demonstrating a truncal artery and aberrant right subclavian artery arising from the descending aorta.

### **Supplemental Movie 9**

Serial axial micro-CT projections through an E17.5 *PlexinD1* mutant mouse embryo reveals an aberrant blood-filled vessel arising from the surface of right ventricular outflow tract and coursing along the left side of the truncal artery as it travels to towards the left superior vena cava.



E17.5

